

# Synthesis and characterization of macroporous sodium alginate-*g*-poly(AA-*co*-DMAPMA) hydrogel

Chengyi Wu<sup>1,2</sup> · Dandan Wang<sup>2</sup> · Huimin Wu<sup>2</sup> ·  
Youmeng Dan<sup>2</sup>

Received: 8 November 2015 / Revised: 16 February 2016 / Accepted: 22 March 2016 /  
Published online: 31 March 2016  
© Springer-Verlag Berlin Heidelberg 2016

**Abstract** In this manuscript, the novel sodium alginate-*g*-poly [acrylic acid-*N*-(3-dimethylaminopropyl) methyl acrylamide] [NaAlg-*g*-P(AA-*co*-DMAPMA)] hydrogel was prepared using free radical polymerization. Fourier transform infrared spectroscopy (FT-IR), thermogravimetry (TG), point zero charge and scanning electron microscopy were used to investigate the structure, thermal stability, surface charge and microstructure of the hydrogel. The factors that affected the swelling ratio of the hydrogel were investigated in detail, such as pH and ionic strength; the results showed that the hydrogel has a favorable pH-sensitive property. To investigate drug loading and sustained release of NaAlg-*g*-P(AA-*co*-DMAPMA), rhodamine B as a model drug was loaded on NaAlg-*g*-P(AA-*co*-DMAPMA). The in vitro drug release study conducted at pH 1.86 and 6.86 shows that NaAlg-*g*-P(AA-*co*-DMAPMA) was suitable for colon-specific drug delivery systems.

**Keywords** Hydrogel · Sodium alginate · Swelling · Controlled release

## Introduction

Hydrogel is a kind of three-dimensional (3D) cross-linked network polymer formed via hydrogen bonding, van der Waals force, chemical bond or physical entanglement. It has many excellent properties, for example, super absorbent capacity, good biological compatibility and biodegradability. So now, hydrogel has attracted more and more attention for researchers as a novel biomaterial [1–4].

---

✉ Chengyi Wu  
wcygfz@126.com

<sup>1</sup> Key Laboratory of Biologic Resources Protection and Utilization of Hubei Province, Enshi, Hubei 445000, China

<sup>2</sup> Department of Chemistry and Environmental Engineering, Hubei University of Nationalities, Enshi, Hubei 445000, China

Intelligent hydrogel is a kind of polymer which has a response to external stimuli, including pH, ionic strength and temperature change [5, 6]. This material was used in many different fields, such as drug delivery, tissue engineering, wound repairing and waste treatment in the textile industry. Intelligent hydrogel that was used as a controlled drug release carrier has many advantages, such as it could deliver drug to the target site in a manner that maximizes its efficacy and minimizes the potential negative effects to other tissues [7, 8]. Natural polymer-based drug delivery devices are a kind of important biomedical material, while sodium alginate (NaAlg) is a natural polysaccharide obtained from kelp or seaweed, composed of (1-4)-linked  $\beta$ -D-mannuronic acid and  $\alpha$ -L-guluronic acid in a non-regular manner. The  $-\text{COOH}$  contained in the chain segment could ionize in alkaline condition. This results in the extension of the molecular chain and did not ionize in acid condition. NaAlg has been widely explored in the biomedical field as a drug carrier [9, 10]. The NaAlg molecular chain contains many carboxyl and hydroxyl residues, which makes it possess the character of better strength to form the polyelectrolyte complexes with the polycation [11].

Due to the good biocompatibility and biodegradability, NaAlg has been widely used as a drug carrier material; however, the main drawback of the gel based on NaAlg was the weak strength and stability. To overcome this weakness, chemical modification methods have been used by graft polymerization on NaAlg [12]. Lang et al. [13] reported that the core-shell structure was prepared with PNIPAAm as the core and sodium alginate as shell. Liu et al. [14] reported that semi-interpenetration of the network hydrogel was done by free radical polymerization, using (2-dimethylamino) ethyl methacrylate (DMAEMA) and glycidyl methacrylate (GMA) as monomers.

The purpose of this manuscript is to overcome the drawbacks of NaAlg hydrogel by forming the hybrid hydrogel through chemical cross-linking. The effect of pore-forming agent type on swelling properties was reported by an investigator [15], especially volume phase transition behavior and response dynamics of poly(*N*-[3-(dimethylaminopropyl)]methacrylamide-*co*-acrylamide) [P(DMAPMA-*co*-AAm)] hydrogel. In this study, a novel pH-sensitive hydrogel was prepared by radical cross-link copolymerization with bi-functional cross-linker *N,N'*-methylenebisacrylamide (MBA) and monomers, DMAPMA and AA. Surprisingly, compared to other hydrogels prepared by other monomers and chemical cross-linkers, this hydrogel exhibits superior swelling capacity, good thermal stability and pH sensibility. Furthermore, RHB was used as a model drug to study their drug release properties. The effect of pH on drug release kinetics was also studied.

## Experiment section

### Materials

Sodium alginate (NaAlg,  $M_w$ :  $4.2 \times 10^5$ ) and acrylic acid (AA) were purchased from Tianjin Chemical Reagent Co. Ltd. *N,N'*-Methylenebisacrylamide, ammonium persulfate, sodium hydroxide, hydrochloric acid, Rhodamine B (RHB) and *N*-(3-amino propyl) dimethyl methyl acrylamide were purchased from Guoyao Chemical

Reagent Co., Ltd. Other reagents were of analytical grade and used without any purification.

### Preparation of NaAlg-g-P(AA-co-DMAPMA)) hydrogel

Hydrogels were prepared by free radical cross-link copolymerization of AA and DMAPMA in aqueous solution of NaAlg and MBA as cross-linker comonomer (as shown in Fig. 1). The polymerization reaction was carried out in a conical flask with

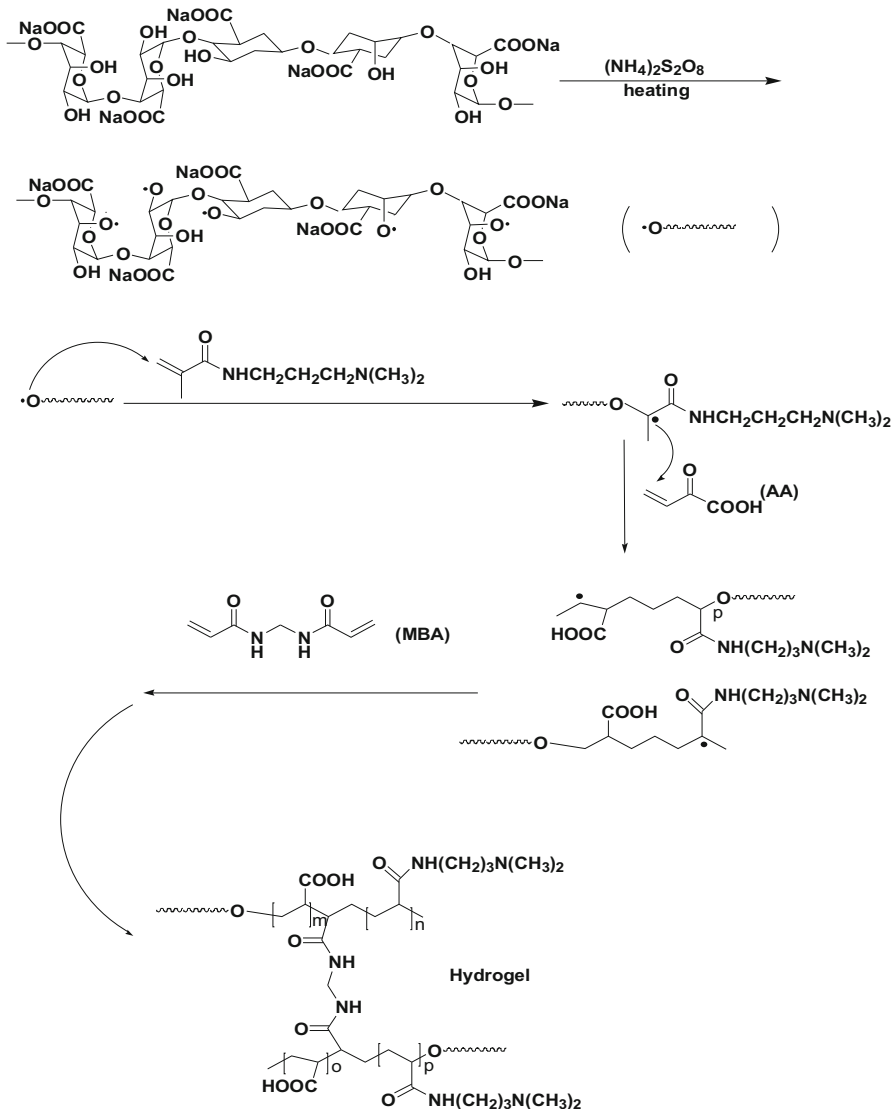


**Fig. 1** The proposed reaction mechanism for the synthesis of NaAlg-g-P(AA-co-DMAPMA) hydrogel

**Table 1** Relative composition of the monomers for the preparation of NaAlg-g-P(AA-co-DMAPMA) systems

Sample	Monomers			Yield (%) <sup>a</sup>
	NaAlg (g)	AA (g)	DMAPMA (g)	
SP-1	0	5	5	53.2
SP-2	0.5	5	5	58.4
SP-3	1	5	5	56.7
SP-4	1.5	5	5	56.1
SP-5	2	5	5	53.8
SP-6	2.5	5	5	54.6

<sup>a</sup> Yield (%) =  $(W_2/W_1) \times 100$  %, where  $W_2$  and  $W_1$  are the dried weights of the washed and unwashed gels

a mechanical stirrer, reflux condenser and thermometer. NaAlg was dissolved in 50 mL water followed by the addition of monomers to this viscous solution and stirring for about 30 min. The dissolved oxygen of the reaction mixtures was removed by purging  $N_2$  before the addition of a certain number of AA, DMAPMA and MBA (as shown in Table 1). The temperature of the reaction mixtures was raised to 60 °C with the addition of ammonium persulfate. The reaction was then continued at this temperature until the reaction mixture gelled, and the hydrogel obtained in long cylindrical shapes was cut into discs of 2 cm diameter and 3 cm thickness. Some hydrogels were washed in distilled water for changing water every 8 h; it needed approximately 1 week to remove the unreacted monomer. The discs were dried to constant weight at 50 °C in a vacuum oven.

### Characterization of the hydrogel

Fourier transform infrared (FT-IR) spectra of the hydrogel were recorded on an FT-IR spectrometer (Perkin Elmer, model-Spectrum-2) using KBr pellet made by mixing KBr with a fine powder of dried samples (20:1 mass ratio of KBr to hydrogel). The morphology of the hydrogel was characterized using scanning electron microscope (Hitachi X650 scanning electron microscope). The samples were dried in a vacuum and placed on an aluminum mount, sputtered with gold palladium and then scanned at an accelerating voltage of 15 kV. Thermogravimetric analysis (TGA) of the samples was carried out in a Mettler instrument in  $N_2$  atmosphere at the rate of 5 °C/min in the range of 25 to 500 °C. UV spectrophotometer (UV-2556) was used to detect the concentration of RHB in solution, and the standard curve equation of RHB was as follows:  $y = 0.0885x - 0.0132$ ,  $R^2 = 0.9994$ .

### Measurement of swelling ratio

The swelling ratio of the hydrogel was measured gravimetrically after sucking the redundant surface water with filter paper, and dry hydrogel was incubated in water at a particular temperature. The swelling ratio is calculated as follows:

$$Q_t = \text{SR}(g/g) = \frac{m_t - m_0}{m_0}, \quad (1)$$

where  $m_t$  and  $m_0$  are the amount of the swollen and dry gel, respectively. To investigate the effect of salinity on the swelling behavior of hydrogel, the dry gel of known mass was immersed in a salt solution containing KCl, CaCl<sub>2</sub> and FeCl<sub>3</sub> in the range from 0.02 to 0.1 mol/L, and then the swelling ratio was calculated using Eq. (1) as mentioned above.

To study the pH sensitivity of the hydrogel, the pH value of acidic and basic solution was prepared by adding 0.1 mol/L HCl or NaOH to obtain the desired pH of 2–12. Then, dry gel samples were immersed in solutions with different pH values and kept for 36 h to attain equilibrium swelling at room temperature. After 24 h, the hydrogel samples were weighed and the swelling ratio was also calculated using Eq. (1).

### Study of drug-loading and entrapment efficiency of the hydrogel

Drug loading and entrapment of hydrogel was carried out as follows: 100 mg purified hydrogel was placed in distilled water for 24 h to reach equilibrium and then soaked in 20 mL aqueous solution of RHB (100 mg/L). Then, the beaker was placed in a stirring bath at 25 °C, after 48 h for adsorption equilibrium, taking out the gel and measuring the volume of solution ( $V$ , mL). The concentrations ( $C$ , mg/L) of the solutions were analyzed by UV spectroscopy at 554 nm to detect the amount of RHB loaded in each hydrogel disc according to the standard curve. The RHB loaded in hydrogel was verified from the difference in the solution concentrations before and after incubation. All experiments were performed in triplicate. Drug loading ( $m$ , mg/g) of hydrogel was calculated by Eq. (2):

$$m = (20 \times 100 - CV) \times 10^{-2}. \quad (2)$$

The hydrogel loaded with RHB were placed in a solution with pH 6.86 and 1.80. The concentration  $m_R$  (mg/L) of RHB in solution was determined by UV spectroscopy. The cumulative release ( $R$ ) was calculated by Eq. (3):

$$R (\%) = (m_R/m) \times 100 \%. \quad (3)$$

### Point zero charge (PZC) analysis

The PZC of hydrogels was measured according to the literature method [16]: 40 mL 0.1 mol/L KNO<sub>3</sub> solution was added to a 250 ml conical flask, the initial pH value ( $\text{pH}_i$ ) of the solution was adjusted by adding 0.1 mol/L HNO<sub>3</sub> or 0.1 mol/L NaOH solution from 2 to 12, and then a certain amount of hydrogel was added and the bottle was covered and vibrated for 48 h at room temperature. The pH value of the final solution ( $\text{pH}_f$ ) was measured. The difference between this initial and final pH ( $\Delta\text{pH} = \text{pH}_i - \text{pH}_f$ ) was plotted against  $\text{pH}_i$  and the point of intersection of the curve at  $\Delta\text{pH} = 0$  gives the value of PZC for the hydrogel.

## Results and discussion

### Mechanism of hydrogel formation

A proposed reaction mechanism for NaAlg-*g*-P(AA-*co*-DMAPMA) hydrogel formation is shown in Fig. 1. In the first step, hydroxyl groups of the NaAlg are converted to the corresponding oxygen free radical with ammonium persulfate at the condition of heating. These oxygen free radicals were used as the initiator, and then the initiator attacked DMAPMA and AA, respectively, forming chain free radicals. The chain free radicals also attacked the monomer, forming new chain free radicals. Meanwhile, MBA was used as a cross-linker to connect the molecular chain. Free radical polymerization proceed until the monomers were consumed. The swelling capacity was strongly dependent on the length of the molecular chain. Therefore, we tried to determine the ratio of NaAlg in the hydrogel under the preparation process.

### Characterization of hydrogel

It was carried out on the FT-IR spectra to confirm the chemical structure of RHB loaded on NaAlg-*g*-P(AA-*co*-DMAPMA)(RHB@NaAlg-*g*-P(AA-*co*-DMAPMA)) (a), NaAlg-*g*-P(AA-*co*-DMAPMA) (b) and NaAlg (c). Figure 2c shows the characteristic absorption bands of NaAlg around 1612 and 1457  $\text{cm}^{-1}$ , which was due to asymmetric and symmetric stretching of the  $-\text{COOH}$  group. A broad peak at 3491  $\text{cm}^{-1}$  is due to the stretching absorption of the hydroxyl groups of the polysaccharide [17]. NaAlg also shows a characteristic peak at 1189  $\text{cm}^{-1}$  corresponding to the O–C–O stretching vibration of the polysaccharide structure. The peak at 559  $\text{cm}^{-1}$  corresponds to the vibration of its Na–O bond. As shown in

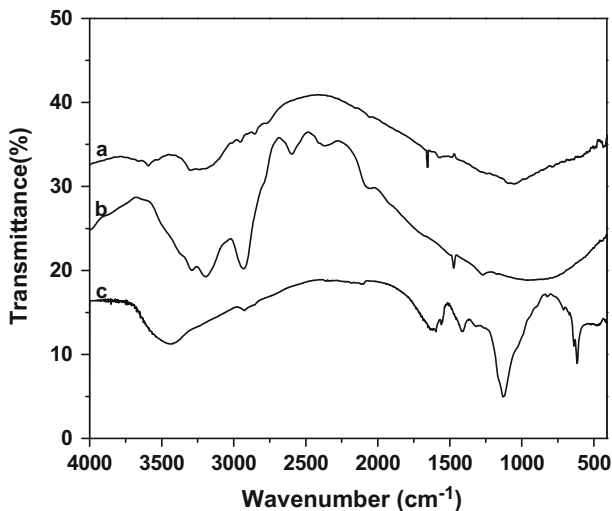


**Fig. 2** FT-IR spectra of *a* RHB@NaAlg-*g*-P(AA-*co*-DMAPMA), *b* NaAlg-*g*-P(AA-*co*-DMAPMA) and *c* NaAlg

Fig. 2(b), the absorption peaks at  $3306$  and  $3154\text{ cm}^{-1}$  correspond to its N–H stretching vibration, while  $1583\text{ cm}^{-1}$  corresponds to its N–H bending [18]. The absorption bands at  $1655\text{ cm}^{-1}$  are due to its C=O stretching. The peak of O–C–O stretching vibration in NaAlg-*g*-P(AA-*co*-DMAPMA) changed less obviously due to overlapping of N–H. The peaks were shifted in drug-loaded NaAlg-*g*-P(AA-*co*-DMAPMA) indicating electrostatic interaction among functional groups of NaAlg and drug-loaded P(AA-*co*-DMAPMA). Similarly, the characteristic peak of benzene ring of RHB at  $1100\text{ cm}^{-1}$  overlapped with the adsorption peak at  $1189$ , and the  $1656\text{ cm}^{-1}$  peak of hydrogel is due to the overlapping of  $-\text{COO}^-$  of NaAlg ( $1612\text{ cm}^{-1}$ ). The model drug RHB shows its characteristic C=N and  $-\text{COOH}$  stretching bands at  $3326$  and  $3162\text{ cm}^{-1}$ , as shown in Fig. 2a. The peak of RHB at  $1560\text{ m}^{-1}$  corresponds to its C=N in plane bending [19].

The TGAs of NaAlg (c), SP-2 (b) and RHB@SP-2 (a) are illustrated in Fig. 3. NaAlg (Fig. 3c) has a two-step degradation temperature, about  $80$  and  $250\text{ }^\circ\text{C}$ . There was about  $15\%$  weight loss at  $80\text{ }^\circ\text{C}$ , due to the evaporation of hydrate water in NaAlg. The maximum degradation temperature was  $250\text{ }^\circ\text{C}$  and the loss weight ratio was  $30\%$ , the reason of which was that the molecular structure of NaAlg degraded at this temperature. However, there was different from SP-2, as shown in Fig. 3b, it was shown that one loss weight regions, which was about  $340\text{--}350\text{ }^\circ\text{C}$ . The thermal stability of the hydrogel increased by about  $100\text{ }^\circ\text{C}$  compared to NaAlg, this was due to the network structure of hydrogel. Figure 3a shows the TG curve of RHB@SP-2, and the different sections compared to Fig. 3b was at  $200\text{ }^\circ\text{C}$  and only  $5\%$  loss weight. The hydrogen bonding interactions between RHB and hydrogel played an important role.

The morphologies of the hydrogel were observed using SEM (as shown in Fig. 4); Fig. 4a shows the surface picture of P(AA-*co*-DMAPMA) and Fig. 4b–d) the morphologies of NaAlg-*g*-P(AA-*co*-DMAPMA) with different weight ratios. Figure 4 shows that there is vesicular structure on the surface of NaAlg-*g*-P(AA-*co*-

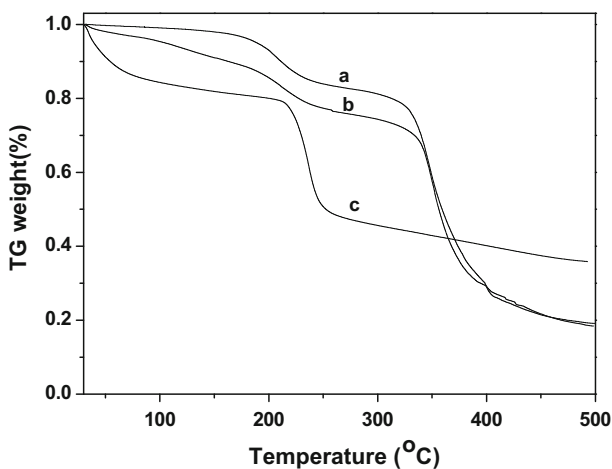


**Fig. 3** TGAs of RHB@SP-2 (a), SP-2 (b) and NaAlg (c)

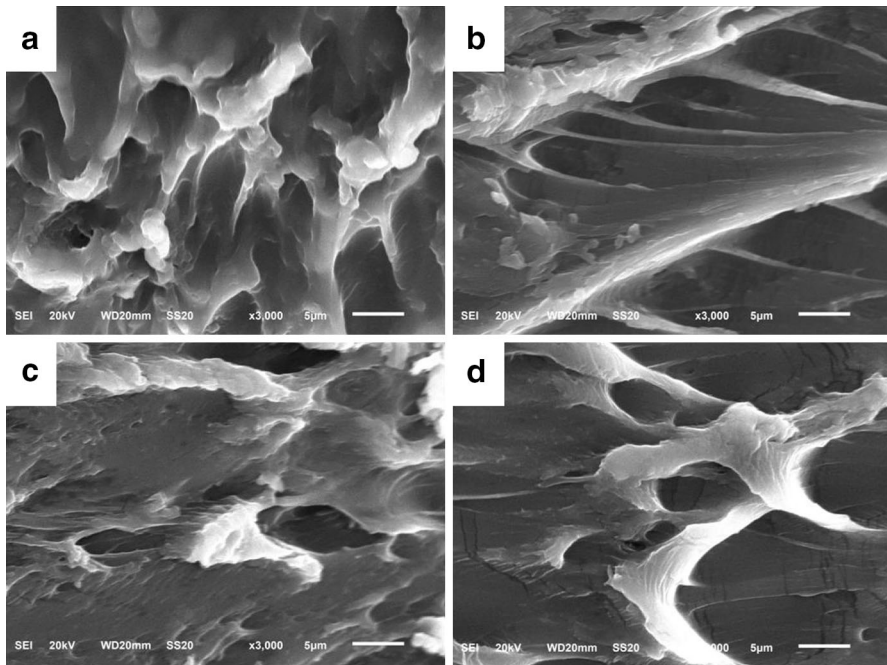


**Fig. 4** SEM micrographs of the surface morphology of SP-1 (a), SP-2 (b), SP-4 (c) and SP-6 (d)

DMAPMA). The porous pattern was more obvious than P(AA-co-DMAPMA), and this increased porosity allows faster water diffusion through the hydrogel network. Moreover, this structure has the benefit of absorbing drug molecules.

### PZC analysis

Testing the surface of the hydrogel was important for their drug delivery application. Not only the drug-loading efficiency of hydrogel, but also their release rates were affected. Suitable surface charge of hydrogel was beneficial to improve the drug release profiles to specific site and patient compliance. Electrostatic interaction between functional groups of drug and surface functionality of hydrogel was the main effect for drug loading. The point of zero surface charge of hydrogel is the pH value ( $\text{pH}_{\text{PZC}}$ ). If  $\text{pH}_{\text{PZC}} = 0$ , the negative and positive surface charges of the hydrogel are equal. If  $\text{pH} > \text{pH}_{\text{PZC}}$ , this means that the surface charge of hydrogel will have a negative value. If  $\text{pH} < \text{pH}_{\text{PZC}}$ , positive, or neutral for  $\text{pH} = \text{pH}_{\text{PZC}}$  [20]. The changes in  $\Delta\text{pH}$  as a function of  $\text{pH}_i$  in 0.1 mol/L  $\text{KNO}_3$  as a background electrolyte are shown in Fig. 5, SP-2 and RHB@SP-2. SP-2 had pH-dependent surface charge due to the presence of the  $-\text{COOH}$  group on their surfaces, which can be ionized or deionized depending on the pH of the solution. The measured  $\text{pH}_{\text{PZC}}$  values depend on the surface composition of hydrogel. Adsorption of RHB on the hydrogel containing AA increases the negative charges on their



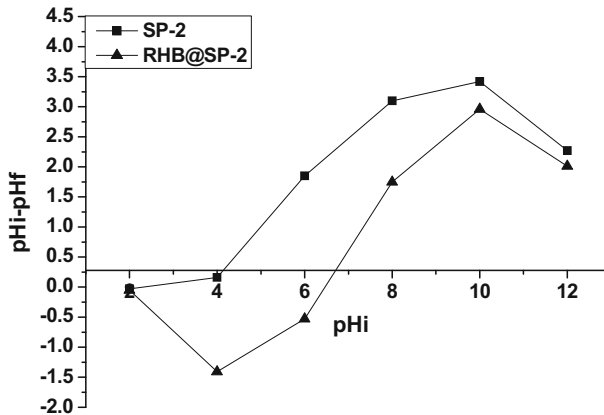


**Fig. 5** PZC analysis of SP-2 and RHB@SP-2

surface. As a result, the  $\text{pH}_{\text{PZC}}$  values of RHB@SP-2 shifted from 4.2 to 6.8. This phenomenon was in accordance with the fact that the specific adsorption of anions shifts the  $\text{pH}_{\text{PZC}}$  toward higher pH values [21].

### Swelling kinetics study

Buchholz et al. [22] have reported that swelling kinetics of hydrogel was affected by several factors, such as swelling ratio, size of material particles and composition of material. Figure 6 illustrates the swelling kinetics of hydrogel in water. The swelling ratio of hydrogel increased with extending time. The swelling equilibrium was reached at about 800 min. The swelling ratio of P(AA-co-DMAPMA) was 70 g/g and that of SP-2 was 107 g/g. This was because the  $-\text{COOH}$  of NaAlg increases the hydrophilicity of the hydrogel. To ensure the nature of diffusion of water into the hydrogel, the following Eq. (4) was used:

$$\frac{M_t}{M_\infty} = kt^n, \quad (4)$$

where  $M_t$  and  $M_\infty$  are the amounts of equilibrium water uptake at time  $t$  and the maximum water uptake, respectively.  $k$  is a proportionality constant and the exponent  $n$  describes the type of diffusion mechanism.  $n$  is 1.0 for the case-II diffusion (relaxation-controlled transport), and for the supercase-II diffusion,  $n$  is greater than 1.0. For non-Fickian or anomalous diffusion,  $n$  is between 0.5 and 1.0. For Fickian diffusion mechanism,  $n$  is 0.5 [23]. A plot of  $\ln(W_t/W_\infty)$  vs  $\ln(t)$  was used to obtain the values of  $n$  and  $k$ . The plot of  $\ln(W_t/W_\infty)$  vs  $\ln(t)$  for the hydrogel samples in water is shown in Fig. 7. Swelling parameter ( $n$ ) and swelling constants ( $k$ ), calculated from the slope and intersect of the lines, respectively, are given in Table 2. As shown in Table 2, the  $n$  values are in the range of 0.5 and 0.90 for the hydrogel, respectively, between 0.5 and 1.0, and illustrated that the transport mechanism was in accordance with non-Fickian diffusion behavior.

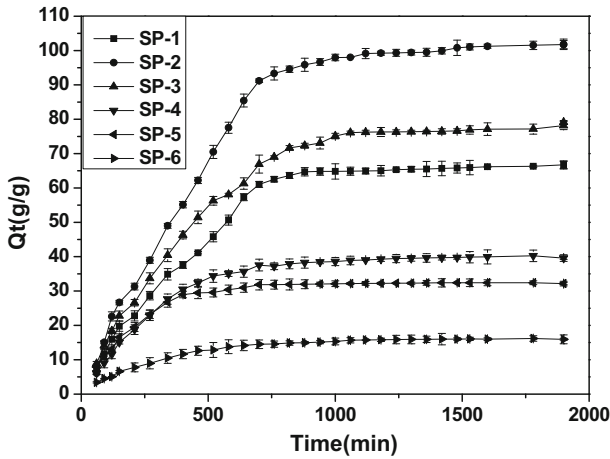


**Fig. 6** Swelling kinetics curve of the hydrogel

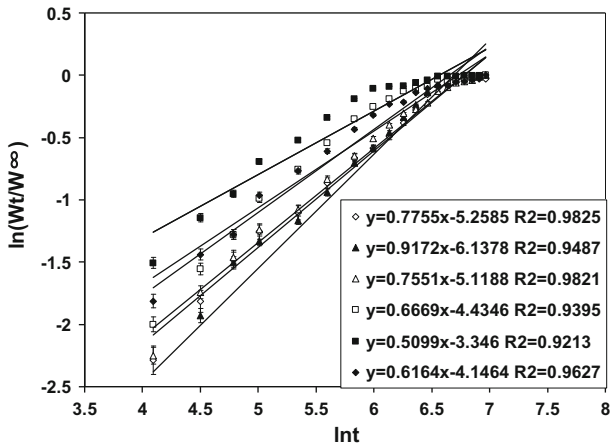


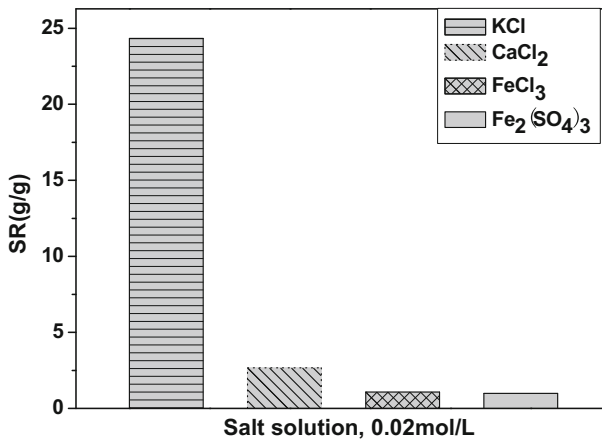
**Fig. 7** Plots of  $\ln(W_t/W_\infty)$  vs  $\ln(t)$  for the hydrogel

### Effect of ionic strength

The swelling ratio of the hydrogel was related to the property of the solution, such as charge number and ionic strength; as well as the structure of the polymer, such as elasticity of the network, hydrophilic group of the polymer and cross-linking density. Generally speaking, the swelling ratio of anionic hydrogel in different salt solutions was lower than that in aqueous solution. This is because of the effect of a certain shielding on the electrostatic repulsive force between anion and anion after cation addition [12]. Figure 8 shows the effect of ionic strength on swelling ratio of

**Table 2** The swelling and diffusion parameters for the hydrogel samples

Sample	<i>n</i>	<i>K</i>
SP-1	0.78	0.0052
SP-2	0.92	0.0023
SP-3	0.76	0.0060
SP-4	0.67	0.0119
SP-5	0.50	0.0352
SP-6	0.62	0.0158

**Fig. 8** Effect of salt solutions on the swelling capacity of the SP-2 hydrogel

hydrogel at the same solution concentration condition. The result shows that the swelling ratio of SP-2 decreases with ionic increase of strength, the reason being that cations have shielding effect to the  $\text{-COO}^-$  of the hydrogel. The effect of cation type on the swelling ratio of the hydrogel is shown in Fig. 9. The results indicated that the swelling ratio decreased with increase in cation charge; this was because the higher the cation type ( $\text{Fe}^{3+} > \text{Ca}^{2+} > \text{K}^+$ ), the more the complexes were formed between  $\text{-COO}^-$  of NaAlg and cation, which caused a tight network. The constriction of swelling capacity is that because the osmotic pressure difference between hydrogel networks and the saline media was reduced and the screening effect of cations on negatively charged  $\text{-COO}^-$  groups was increased with increasing the concentration of saline solution. In the solution of multivalent saline, the ionic sites of the hydrogel can complex with multivalent cations, which weakened the negative charges in polymeric chains and produced packed network by ionic cross-linking interaction. As a result, the expansion of the polymeric network was limited and the swelling capacity decreased more obviously [24].

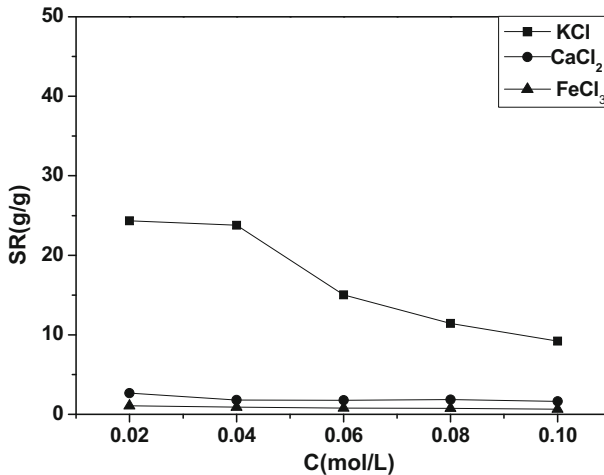


**Fig. 9** Effect of ionic strength on the swelling ratio of the SP-2 hydrogel

### Effect of pH

Generally, ionic hydrogel have pH sensitivity, so the pH of solution decided the swelling ratio of hydrogel. The swelling ratio of SP-2 in the range from 2 to 12 is shown in Fig. 10. The pH of the solution was adjusted by 0.1 mol/L HCl and NaOH, and the maximum swelling ratio (105.41 g/g) was observed at pH 8. The swelling ratio of the hydrogel was only 1.14 g/g at pH 2, the reason was that the ionization of  $-\text{COOH}$  was suppressed and form hydrogen bond, and water molecule did not enter the network hole. The swelling ratio of SP-2 increased from 74.8 to 105.41 g/g at pH 4–8. The reason was that  $-\text{COOH}$  could ionize, and the electrostatic repulsion between the  $-\text{COO}^-$  groups caused an enhancement of the swelling capacity. However, the swelling ratio decreased obviously when pH was above 12. The reason was the charge-screening effect of massive  $\text{Na}^+$  in the swelling media, which shielded the carboxylate anions and prevented effective anion–anion repulsion [25].

### In vitro controlled drug release study

To imitate the condition of stomach and intestine, RHB was employed as a model drug, and the pH 1.86 and 6.86 solutions were prepared for RHB-controlled release. Drug loading (m) of SP-2 was 3.188 mg/g. The morphology of SP-2 is macroporous; such structure is suitable for the adsorption of a higher amount of the drug. Release behavior of RHB in aqueous solution was affected by pH value (as shown in Fig. 11). The cumulative release was only 28 % at 500 min at pH 1.86. However, the cumulative release (R %) reached 70 % at 500 min at pH 6.86. The main reason was that ionization of  $-\text{COOH}$  was restrained, the network hole minimized and RHB did not diffuse from the hydrogel interior. The hydrogel could swell sufficiently so that the drug could diffuse easily at pH 6.86.

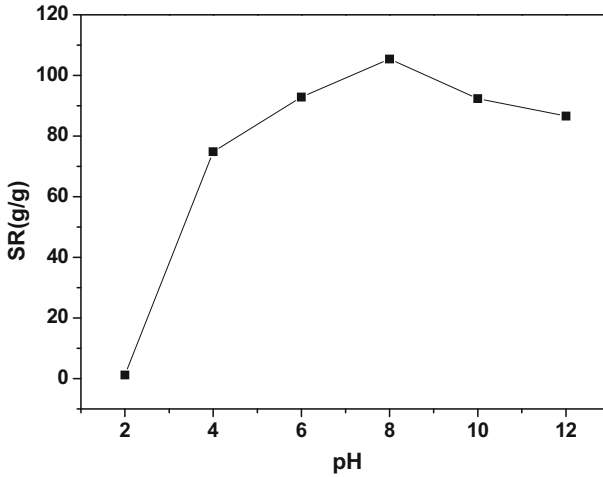


**Fig. 10** Effect of pH on the swelling ratio of the SP-2 hydrogel

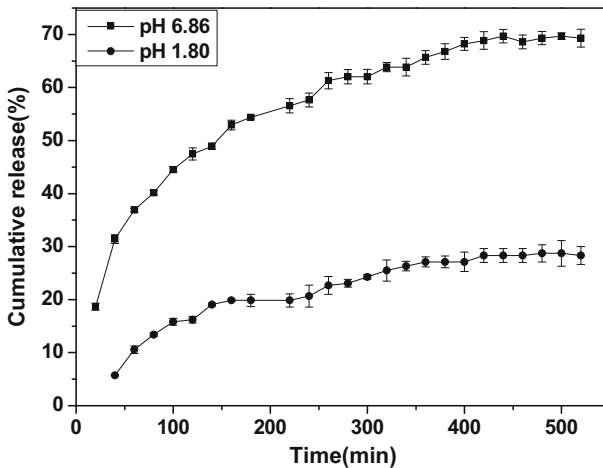


**Fig. 11** In vitro cumulative release profiles of RHB from SP-2 hydrogel at different pH values at 37 °C

### Conclusion

In this study, a macroporous NaAlg-*g*-P(AA-*co*-DMAPMA) hydrogel was prepared by free radical copolymerization and was investigated as matrices for the controlled release of a model drug RHB. The FT-IR was employed to confirm the structure and incorporation of the drug with the hydrogel. SEM images of the hydrogel indicated the porous interior structure which was a benefit to load the drug. The TG curve revealed that the decomposition temperature of NaAlg-*g*-P(AA-*co*-DMAPMA) was in the range of 340–350 °C. The swelling behavior of hydrogel was also

investigated in the pH range (2.00–12.00). The results show that the hydrogel had good pH-sensitive behavior. This means that they are suitable for the site-specific drug delivery for changing pH values. RHB as a model drug was used to investigate the slow release of hydrogel at pH 1.86 and 6.83. The results indicated that the release rate of the drug could be affected by pH changes. The hydrogels prepared in this study are potentially applicable as materials in the fields of bioengineering.

**Acknowledgments** This work has been supported by the Youthful National Science Foundation of Hubei (No. 2014CFB618); the Open Science Foundation of Key Laboratory of Biological Resources Protection and Utilization of Hubei Province (No. PKLHB1511); the Science Research Group of Hubei University for Nationalities (MY2014T007, MY2013T004); the Doctoral Science Research Foundation of Hubei University for Nationalities (MY2013B017).

## References

1. Jaiswai M, Koul V (2013) Assessment of multicomponent hydrogel scaffolds of poly(acrylic acid-2-hydroxy ethyl methacrylate)/gelatin for tissue engineering applications. *J Biomater Appl* 27:848–861
2. Yin W, Su R, Qi W, He Z (2012) A casein-polysaccharide hybrid hydrogel cross-linked by transglutaminase for drug delivery. *J Mater Sci* 47:2045–2055
3. Biswas CS, Sulu E, Hazer B (2015) Effect of the composition of methanol-water mixtures on tacticity of poly (N-ethylacrylamide) gel. *J Appl Polym Sci* 132:41668–41678
4. Khademhosseini A, Langer R (2007) Review: microengineered hydrogel for tissue engineering. *Biomaterials* 28:5087–5092
5. Biswas CS, Hazer B (2015) Synthesis and characterization of stereoregular poly(N-ethylacrylamide) hydrogel by using  $Y(OTf)_3$  Lewis acid. *Colloid Polym Sci* 293:143–152
6. Şanal T, Oruç O, Öztürk T, Hazer B (2015) Synthesis of pH- and Thermo-responsive Poly( $\epsilon$ -Caprolactone-b-4-vinyl benzyl-g-dimethyl amino ethyl methacrylate) Brush Graft Copolymers via RAFT Polymerization. *J Polym Res* 22(3):1–12
7. Jaiswal M, Gupta A, Dinda AK, Koul V (2010) Polycaprolactone diacrylate (PCL-DAR) crosslinked biodegradable semi-interpenetrating networks (semi-IPNs) of polyacrylamide and gelatin for controlled drug delivery. *Biomed Mater* 5:065014
8. Shamunga Sudar S, Sangeetha D (2012) Investigation on sulphonated PEEK beads for drug delivery, bioactivity and tissue engineering applications. *J Mater Sci* 47:2736–2742
9. Rajesh N, Siddaramaiah (2009) Feasibility of xanthan gum–sodium alginate as a transdermal drug delivery system for domperidone. *J Mater Sci Mater Med* 20(10):2085–2089
10. Agnihotri SA, Kulkarni RV, Nadagouda NM, Kulkarni PV, Aminabhavi TM (2005) Electrically modulated transport of diclofenac salts through hydrogel of sodium alginate, carbopol, and their blend polymers. *J Appl Polym Sci* 96(2):301–311
11. Hua S, Ma H, Li X, Yang H, Wang A (2010) pH-sensitive sodium alginate/poly(vinyl alcohol) hydrogel beads prepared by combined  $Ca^{2+}$  crosslinking and freeze-thawing cycles for controlled release of diclofenac sodium. *Int J Biol Macromol* 46(5):517–523
12. Bagheri Marandi G, Sharifnia N, Hosseinzadeh H (2006) Synthesis of an alginate- poly(sodium acrylate-co-acrylamide) superabsorbent hydrogel with low salt sensitivity and high pH sensitivity. *J Appl Polym Sci* 101:2927–2937
13. Lang YY, Jiang TY, Li SM, Zheng LY (2008) Study on physicochemical properties of thermosensitive hydrogel constructed using graft-copolymers of poly(N-iso-propylacrylamide) and guar gum. *J Appl Polym Sci* 108(6):3473–3479
14. Gao CM, Liu MZ, Chen J, Chen C (2012) pH- and temperature-responsive P(DMAEMA-GMA)-Alginate semi-IPN hydrogel formed by radical and ring-opening polymerization for aminophylline release. *J Biomat Sci Polym E* 23:1039–1054
15. Demirel GB, Caykara T, Demiray M, Gürü M (2009) Effect of pore-forming agent type on swelling properties of macroporous poly(N-[3-(dimethylaminopropyl)]-methacrylamide-co-acrylamide) hydrogel. *J Macromol Sci Part A Pure Appl Chem* 46:58–64

16. Mall ID, Srivastava VC, Kumar GVA, Mishra IM (2006) Characterization and utilization of mesoporous fertilizer plant waste carbon for adsorptive removal of dyes from aqueous solution. *Colloid Surf A* 278:175–187
17. Kulkarni RV, Sreedhar V, Mutalik S, Setty CM, Sa B (2010) Interpenetrating network hydrogel membranes of sodium alginate and poly(vinyl alcohol) for controlled release of prazosin hydrochloride through skin. *Int J Biol Macromol* 47:520–527
18. Zhou C, Wu Q (2011) A novel polyacrylamide nanocomposite hydrogel reinforced with natural chitosan nanofibers. *Colloids Surf B* 84:155–162
19. Pachuaua L, Mazumder B (2012) *Albizia procera* gum as an excipient for oral controlled release matrix tablet. *Carbohydr Polym* 90:289–295
20. Wang XF, Sun XW, Liu WX, Gong BY, Gao NB (2008) Chitosan hydrogel beads for fulvic acid adsorption: behaviors and mechanisms. *Chem Eng J* 142:239–247
21. Pechenyuk SI (1999) The use of the pH at the point of zero charge for characterizing the properties of oxide hydroxides. *Russ Chem B* 48:1017–1023
22. Buchholz FL, Fredric L, Peppas NA (eds) (1994) Superabsorbent polymers: science and technology: developed from a symposium sponsored by the division of polymeric materials: science and engineering. ACS Symposium Series 573. American Chemical Society, Washington, DC
23. Kasgoz H, Durmus A (2008) Dye removal by a novel hydrogel-clay nanocomposite with enhanced swelling properties. *Polym Adv Technol* 19:838–845
24. Gao TP, Wang WB, Wang AQ (2011) A pH-sensitive composite hydrogel based on sodium alginate and medical stone: synthesis, swelling, and heavy metal ions adsorption properties. *Macromol Res* 19(7):739–748
25. Park SE, Nho YC, Lim YM, Kim H (2004) Preparation of pH-sensitive poly(vinyl alcohol-*g*-methacrylic acid) and poly(vinyl alcohol-*g*-acrylic acid) hydrogel by gamma ray irradiation and their insulin release behavior. *J Appl Polym Sci* 91:636–643